https://www.scirp.org/journal/ns Natural Science, 2025, Vol. 17, (No. 11), pp: 173-186

Experimental and Computational Study of Amino Acid Synthesis from Acetonitrile and Glycine Oligomers on a Carbonate Surface under UV-C Radiation: Implications for Titan and Early Earth

Karina Rosario Ortiz Leyra[1,2,3,4], **Alejandro Heredia Barbero**[1,2,3]

[1]Laboratorio de Evolución Química, Departamento de Química de Radiaciones y Radioquímica, Instituto de Ciencias Nucleares, Ciudad de México, México; [2]The Network of Researchers on the Chemical Evolution of Life Institute (The NoRCEL Institute), Leeds, UK; [3]Sigma Xi, The Scientific Research Honor Society, North Carolina, USA; [4]Sociedad Mexicana de Astrobiología (SOMA), Ciudad de México, México

Correspondence to: Karina Rosario Ortiz Leyra, karina.ortiz@correo.nucleares.unam.mx; Alejandro Heredia Barbero, aheredia@correo.nucleares.unam.mx

Keywords: Early-Earth, Titan, Prebiotic, Aminoacids, Tholins

Received: November 6, 2025 **Accepted:** December 20, 2025 **Published:** December 23, 2025

ABSTRACT

This study investigates prebiotic chemistry on Titan and Early Earth using experimental methods, including Differential Scanning Calorimetry (DSC) and Fourier-Transform Infrared Spectroscopy (FTIR), which are relevant for identifying molecular structures and thermal stability of amino acids. Analyses of glycine and acetonitrile with calcium carbonate under UV-C radiation show that glycine oligomers facilitate stable amino acid synthesis. We conclude that Titan's environment can directly support the formation of life-relevant molecules, revealing a plausible pathway for chemical evolution analogous to that on Early Earth.

1. INTRODUCTION

Amino acids are crucial in astrobiology, with at least 300 identified, but only 20 are primarily relevant for protein synthesis in living organisms [1]. The concept of searching for these amino acids in prebiotic environments is rooted in foundational experiments such as the Alfonso Luis Herrera [2] and Miller-Urey experiments [3], which synthesized prebiotic compounds from simple molecules present in possible Early Earth conditions [4]. This research suggests the possibility of analogous environments, such as Titan, which was explored by the Cassini-Huygens mission [5], and may serve as natural laboratories for the formation of complex prebiotic compounds [6]. Peptide bonds, known for their stability and linear structure, form between amino acids through covalent bonding. Linus Pauling made significant contributions to understanding protein structure and bonding characteristics [7]. Furthermore, minerals on Earth are potential

catalysts for amino acids and other small-molecule reactions, particularly under ionizing radiation. For astrobiology and molecular evolution studies, different ionizing radiations should be considered [8]. Among the ancient amino acids, Glycine, like other compounds, exhibits changes when subjected to gamma radiation [9], which may enhance interactions among amino acids and contribute to the emergence of new properties [10]. These catalytic reactions, primarily influenced by ubiquitous minerals such as carbonates, can lead to both structural stability and the formation of organic molecules [11]. In these conditions, it seems that Titan and ancient Earth share some similarities [12]. The complex catalytic phenomena might have formed molecular machines on ancient Earth [13, 14], thereby increasing biological complexity. However, their instability prompts research aimed at enhancing their stability, with studies suggesting that increasing the molecular mass of amino acids, such as glycine, may offer physicochemical versatility [15]. In Titan's atmosphere, the abundance of methane and molecular nitrogen, together with UV-C radiation and cosmic rays, drives the formation of tholines in its stratosphere, located around 100 km above the surface. The Urey-Miller experiment indicated that tholines formed on Early Earth are precursors to essential biological molecules, including amino acids and nucleic acids [16]. Laboratory simulations have identified that tholines exhibit aerosol-like behavior, contributing to Titan's reddish coloration [17]. Amino acids produced from tholines are potential bioindicators for environments conducive to prebiotic chemistry, suggesting the possibility of complex molecule formation, such as proteins, on Titan. It has been noted that tholines react to produce amino acids at approximately 1000 km in Titan's atmosphere, with molecular evolution occurring at altitudes of around 2000 km [18].

Carbonates on Titan provide insights into conditions that could facilitate molecular evolution, similar to those on Early Earth. Acetonitrile, found in both Titan's atmosphere and in extraterrestrial environments, suggests its significance in Early Earth conditions. Both Titan and Early Earth are subjected to ionizing radiation from solar sources, which plays a crucial role in electron activation within molecules. This type of radiation, including UV-C [19, 20], travels through various media and has implications for chemical processes. Recognizing these planetary conditions emphasizes their relevance for understanding prebiotic chemistry and guides future[21]directions.

This work reports the synthesis of amino acids and other oligomers of amino acids from mixtures of glycine up to hexaglycine and oligomers under simulated Titan and Early Earth conditions using acetonitrile, calcite, and UV-C radiation. While these conditions aim to replicate planetary environments, limitations such as the scale and duration of experiments are acknowledged. Reaction products are analyzed via polarized microscopy, DSC, FTIR spectroscopy, and HyperChem simulations to assess prebiotic potential and compare planetary environments such as organic characterization—Primitive Earth: presence of atmospheric acetonitrile, anaerobic oxidation of methane [4], presence of water [22]; formation of amino acids (Criado-Reyes *et al.*, 2021). Titán: atmosphere with methane, acetonitrile, and water [23, 24]; formation of tholins [25]; presence of amino acids [26]. Inorganic Characterization—Primitive Earth: presence of surface carbonates [27]; solar radiation (X-ray) and ultraviolet radiation [28]. Titan: presence of surface carbonates [29]; ultraviolet light, cosmic rays [17] and bolide impacts [30]. These factors influence the extrapolation of laboratory results to planetary conditions and are discussed in the context of their limitations.

2. METHODOLOGY

In our model of molecular evolution [31], the oligomerization of amino acids (Gly1 G-7126, Gly2 G-1002, Gly3 G-1377, Gly4 G-3882, Gly5 G-5755, Gly6 G-5630, Merck group®, Burlington, Massachusetts, EEUU) and formation of other relevant prebiotic compounds through hydration and dehydration processes with acetonitrile is a co-adjuvant process. To assess the relevance of UV-C radiation, single crystals of Island spar ($CaCO_3$, Mineralia®, Coyoacán, Mexico City) and CH_3CN (J.T.Baker® brand chemistries. MW: 41.05 g/mol. Avantor, Pennsylvania, EEUU) in the stability and synthesis of compounds under primitive Earth and Titan conditions, samples were prepared in solid and aqueous solution. These samples were irradiated with UV-C (Pen lamp Fisher Scientific Pen Ray LAMP UVP, UVC, Ace Glass, model PS-1 115 V - 60 Hz,

primary energy of 254 nm, Pittsburgh, EEUU, and a UV-C Flow Cabinet Ecoshel, model CV-1, with a primary emission of 253.7 nm, Pharr, Texas) for 3 hours, with removal of samples every half hour at a constant distance of approximately 5 to 15 mm.

2.1. Computational Simulations with Hyperchem with the MM+ and PM3 Levels of Theory for Geometry Optimization and Molecular Dynamics

Computational modeling was employed to achieve an optimal balance between accuracy and computational cost in studying oligomer-mineral interactions. The MM+ force field was selected for initial geometry optimization and molecular dynamics simulations due to its proven efficacy in modeling large, structured organic-inorganic interfaces. Its parametrization for potential energy calculations, including van der Waals forces, electrostatic interactions, and torsion energies, is particularly suitable for simulating the adsorption and adhesion of glycine oligomers onto the calcite ($CaCO_3$) surface, providing a robust structural foundation. Molecular dynamics further relaxed the system by sampling conformational space through atomic vibrations, helping to locate a global energy minimum and ensuring structural stability [32]. Subsequently, the PM3 semi-empirical method was applied to the optimized structures, as it incorporates quantum-mechanical electron effects at a feasible computational cost. This allows for the determination of molecular interaction sites and assessment of potential chemical reactivity by accounting for electron distribution and core repulsion, which is essential for understanding charge transfer and polarization at the oligomer-calcite interface. For both MM+ and PM3, the Polak-Ribiere conjugate gradient algorithm was used with a root mean square gradient of 0.001 kcal·mol^{-1}. This combined methodology ensures both efficient conformational sampling and electronic insight, making it highly appropriate for systems where organic molecule-mineral surface interactions play a defining role.

2.2. Polarized Light Microscopy

Light is a form of electromagnetic radiation composed of photons. Therefore, it can be used to study the changes that occur when a material is exposed to a light source. To use polarized light, the polarizers adapted to the microscope (SMART-POL Drawell, Chongqing, China) are exchanged so that the birefringent effect exposes the characteristics of the studied materials. The microscope is coupled to a digital camera to obtain different images.

2.3. Differential Scanning Calorimetry (DSC)

Heating was constant at a rate of 20˚C /min, in a static air atmosphere with aluminum crucibles. DSC's purpose is to characterize the stability of compounds (ΔH, ec. 1) and induce the state of structural relaxation in molecules [33]. For sample analysis, the instrument (DSC-100 Tryte Technology, Hunan Development Co., Ltd, Yuhua District, Changsha, Hunan, China) has a heating cell containing two sensors where a reference crucible and a crucible with the sample are placed, in addition to a control panel where the parameters under which the sample will be analyzed are configured.

$$Cp = \left(\frac{\Delta H}{\Delta T}\right)_p \rightarrow \Delta H = \int_{T_1}^{T_2} Cp_{p,ex} dT \quad (1)$$

2.4. Attenuated Total Reflectance Fourier-Transform Infrared Spectroscopy ATR-FTIR

Infrared spectroscopy determines the components and structure of molecular samples through their vibrational spectra, yielding bands corresponding to specific functional groups. As a non-destructive analysis tool, it allows samples to be recovered at different times during their analysis. A beam of light emitting in the entire infrared region is incident on a beam splitter that divides it into two beams of equivalent energy, one of which is incident on a movable mirror and the other on a fixed mirror. The beams are recombined, and the resulting beam is emitted towards the sample, which absorbs the wavelengths and

emits them to the detector, producing a spectrogram with the bands emitted by the irradiated sample [34]. In this study, an ATR-FTIR PerkinElmer 100 FT-IR spectrometer (Shelton, CT, USA) equipped with universal fully attenuated reflectance sampling and a zinc selenide sample holder was used. IR spectra were recorded in the range 4000 cm^{-1} to 650 cm^{-1} with a resolution of 4 cm^{-1} and four scans per sample.

The Second Derivative Method to Increase the Resolution of the Infrared Spectra

One way to gain insight into the signals in more detail from the FTIR spectra is by applying the second derivative (ec. 2), which can evidence small changes in the vibrational behavior from the education for derivatives:

$$\frac{d^2T(f)}{df^2} \approx \frac{T(f+\Delta f)-2T(f)+T(f-\Delta f)}{(\Delta f)} \quad (2)$$

After using the second derivative, the small changes of the band will be revealed, showing the differences among bands [35]. These visual changes can provide information about the most reactive intervals in the spectrogram; therefore, we can focus on this to interpret the results.

3. RESULTS

3.1. Computer Simulations

Our computer simulations revealed varying energy levels associated with the formation of secondary structures, which are significant due to their emergent properties, particularly in catalysis and organic synthesis. The results indicate that the β-sheet exhibits a total energy of −44.964 kcal·mol^{-1}, while the α-helix has an energy of −26.0187 kcal·mol^{-1}. This suggests that the β-sheet is the more stable configuration, as it demonstrates lower energy after optimization through geometry and molecular dynamics. Such thermodynamic properties, which favor the β-sheet, could provide a foundation for synthesizing this structure with catalytic capabilities akin to those of a molecular machine [36] (**Figure 1**).

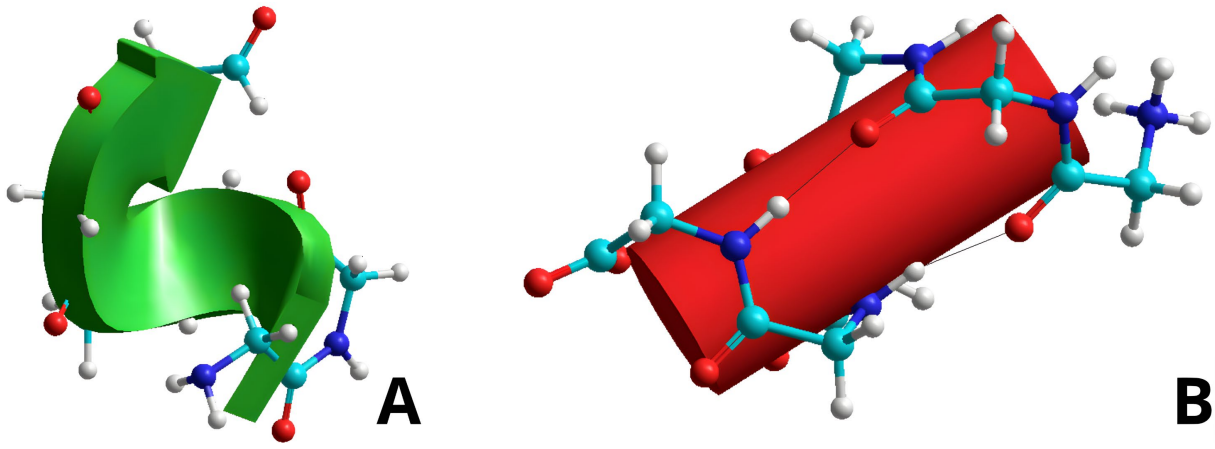

Figure 1. Secondary structure of glycine (MM+) oligomers (A) β-sheet and alpha-helix (B).

The simulation of oligomer secondary structures was conducted using calcite and acetonitrile. Results indicate that structures incorporating calcite exhibit an energy weakening pattern, with energy increasing from 1Gly to 4Gly and decreasing in 5Gly, suggesting a stabilization effect. Conversely, for calcite with acetonitrile, the dipole moment shows an increase from 1Gly to 4Gly but decreases at 5Gly, highlighting differences in behavior compared to amino acids on the surfaces of these substances. The semiempirical PM3 method was employed after the MM+ simulations, utilizing a single-point method to maintain atomic positions, as shown in **Table 1**, **Table 2**, and **Table 3**.

Table 1. Values obtained from computational simulations showing the potential energy values and dipole moments in MM+ and PM3 methods for control glycines.

Simulation	MM+ energy (kcal·mol^{-1})	Dipole moment (D)	PM3 energy (single point*) (kcal·mol^{-1})	Dipole moment (D)
Gly	5.650	3.267	−892.151	10.64
2Gly	11.887	5.31	−1640.39	7.076
3Gly	16.372	1.546	−2376.08	9.081
4Gly	22.886	3.541	−3163.66	13.15
5Gly	26.137	3.962	−3904.12	9.361
6Gly	29.022	5.557	−4750.23	10.37

Table 2. Values obtained from the computational simulations showing the dipole energies and dipole moments in MM+ and PM3 methods with $CaCO_3$.

Simulation	MM+ energy (kcal·mol^{-1})	Dipolar moment (D)	PM3 energy (single point*) (kcal·mol^{-1})	Dipolar moment (D)
Gly + $CaCO_3$	41.164	3.29	264,308	5916
2Gly + $CaCO_3$	50.534	4.444	371,444	6276
3Gly + $CaCO_3$	53.716	2.687	1,900,860	19,230
4Gly + $CaCO_3$	55.570	2.608	2,139,180	18,650
5Gly + $CaCO_3$	57.125	4.00	2,339,850	19,330
6Gly + $CaCO_3$	57.256	7.27	2,557,890	20,760

Table 3. Values obtained from the computational simulations showing the dipole energies and moments in MM+ and PM3 methods with $CaCO_3$ and CH_3CN.

Simulation	MM+ energy (kcal·mol^{-1})	Dipole moment (D)	PM3 energy (single point*) (kcal·mol^{-1})	Dipole moment (D)
Gly + $CaCO_3$ + CH_3CN	41.733	0.3	650,812	6498
2Gly + $CaCO_3$ + CH_3CN	54.821	2.92	835,594	8949
3Gly + $CaCO_3$ + CH_3CN	72.505	1.258	2,569,810	18,480
4Gly + $CaCO_3$ + CH_3CN	129.568	4.327	2,776,970	23,020
5Gly + $CaCO_3$ + CH_3CN	69.135	3.876	2,612,860	19,780
6Gly + $CaCO_3$ + CH_3CN	115.517	8.775	3,215,540	22,590

*Energy calculation without readjusting the structural optimization.

In the simulations of oligomerizations, the formation of one water molecule per peptide bond is accounted for, resulting in the generation of five water molecules in the hexaglycine model (Figure 2).

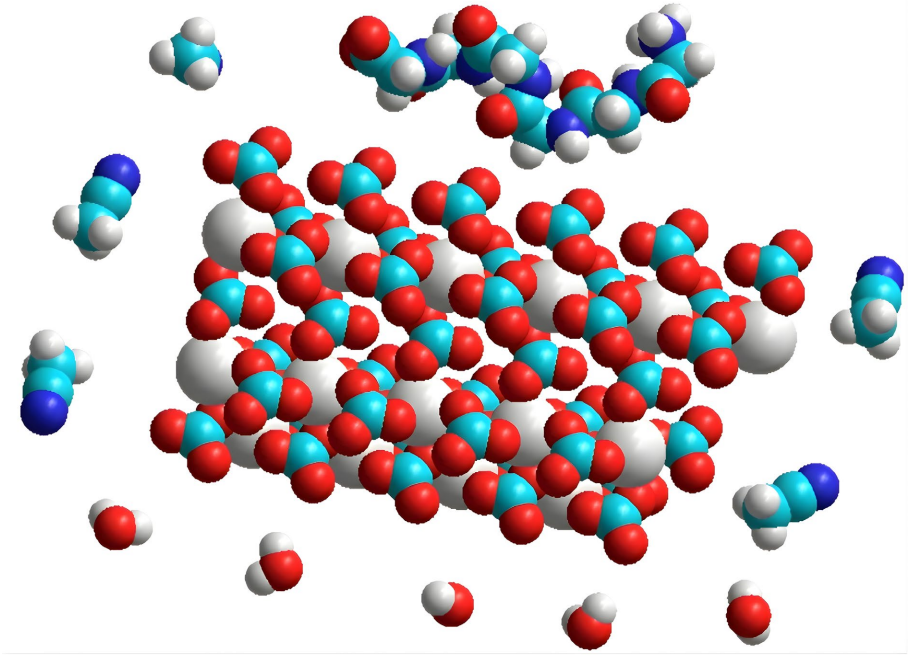

Figure 2. MM+ computational simulation of the interaction of hexaglycine, calcite, and acetonitrile with five water molecules. The values for this simulation are 6.26 kcal·mol^{-1} energy and 5.315 Debyes dipole moment.

3.2. Polarized Light Microscopy

Figure 3 illustrates a rhombohedral exfoliated $CaCO_3$ crystal, featuring distinct crystalline planes that facilitate its interaction with irradiated glycines. The images highlight unpolarized regions within the oligomers (Figure 4), indicating the presence of high-molecular-mass compounds.

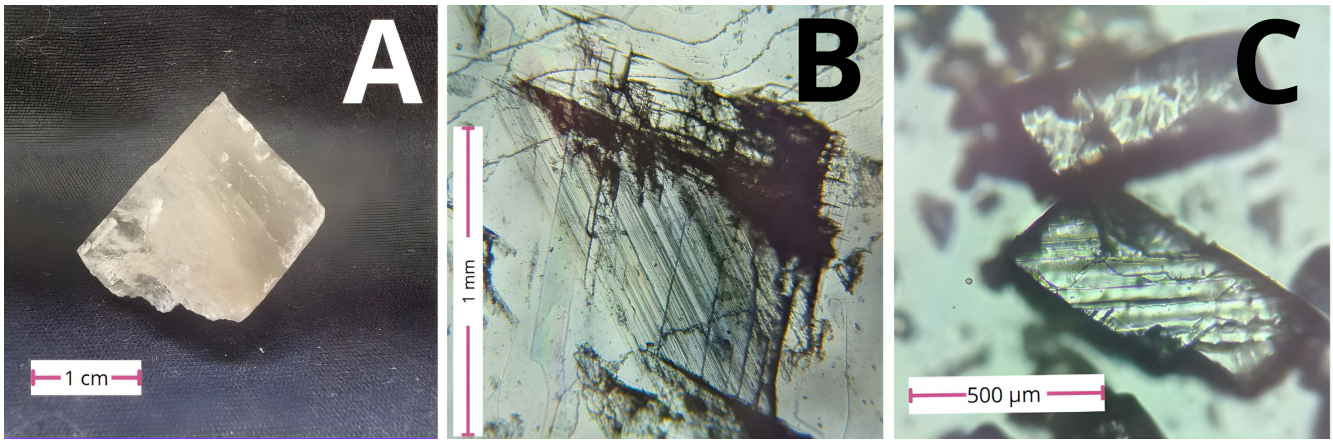

Figure 3. Samples of Iceland spar single crystals at different scales. (A) Iceland spar with the naked eye, with visible linear fractures (B), (C). Optical microscopy view of Iceland spar sample showing the characteristic rhombohedral fracture of calcite.

Figure 4 depicts glycine, characterized by rounded edges and opacity under polarized light (4A). In contrast, Figure 4(B) identifies calcite by its angular edges and clear diaphaneity in polarized light. The addition of glycine to the carbonate is evident in Figure 4(C), where the 1Gly mixture allows light to penetrate various areas, revealing the distinct identities of calcite and glycine. Figure 4(D) shows 6Gly, illustrating a more pronounced interaction, with observable glycine adhering to the calcite crystal surface.

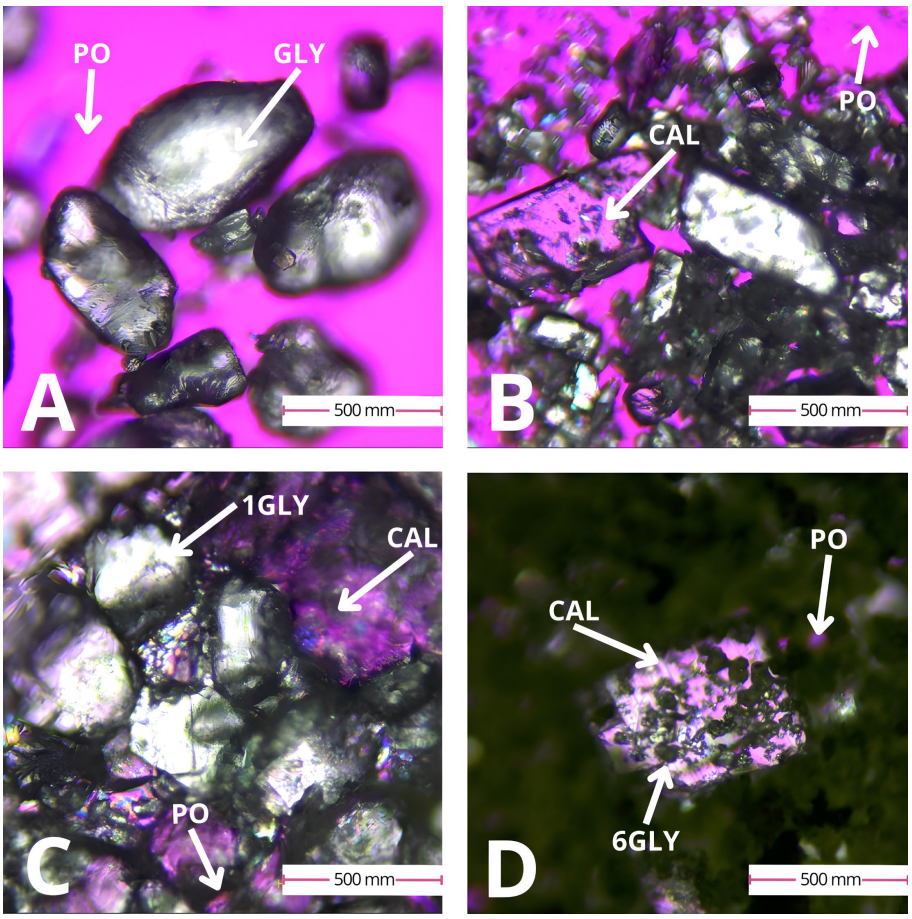

Figure 4. Dehydrated samples were analyzed under polarized light microscopy. (A) Glycine; (B) $CaCO_3$; (C) $CaCO_3$+ Glycine; (D) $CaCO_3$+ 6Glycine. In the image, the glass slide corresponds to (PO), calcite to (CAL), and glycines to (1GLY, 6GLY).

3.3. Differential Scanning Calorimetry (DSC)

For the experiment in Differential Scanning Calorimetry (DSC) without exposure to UV-C irradiation (Figure 5), glycine samples 1 through 5 displayed endothermic curves, whereas hexaglycine exhibited three exothermic peaks, indicating distinct thermal behaviors. The enthalpy changes represented in the thermograms correspond to the relaxation, formation, or breakdown of the compounds, with endothermic processes (positive ΔH values) and exothermic processes (negative values). The thermal transitions of glycine up to pentaglycine show a relatively consistent increase, whereas hexaglycine's exotherms suggest the presence of a secondary structure within the oligomer. The thermal transitions for glycine samples with $CaCO_3$ are noted, with hexaglycine showing all three exothermic values again. Interestingly, samples with $CaCO_3$ and CH_3CN exhibited endothermic transitions at lower temperatures, indicating a significant loss of stability as the thermal transitions decreased from approximately 300˚C to around 100˚C. Multiple curves were recorded per analysis, and averages were used for improved data management.

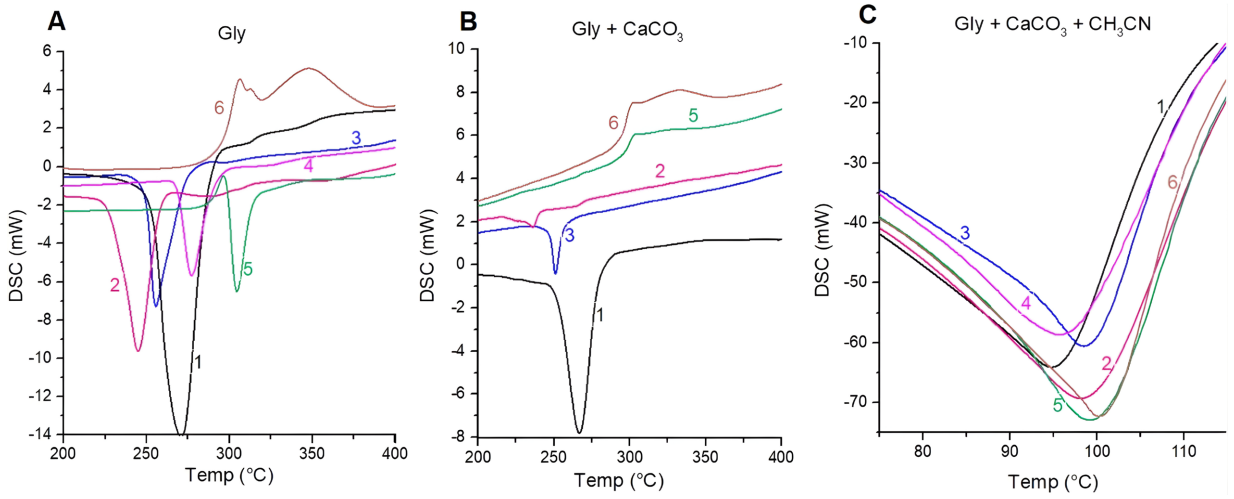

Figure 5. Differential scanning calorimetry plots of the different glycine samples are shown in colored curves, from 1Gly to 6Gly, corresponding to their oligomers, where A represents the glycine samples, B represents those with added $CaCO_3$, and C represents those with added CH_3CN to simulate a molecular evolution process.

The graphical representations of enthalpy and transition temperatures reveal significant findings. In Figure 6(A), negative values indicate low energy requirements for reactions, with the highest enthalpy observed in the mixtures of Gly with 4Gly and 5Gly. Figure 6(B) shows that the lowest thermal temperature occurs at 2Gly, while the highest is at 6Gly. Overall, Gly exhibits the highest thermal transition temperature, whereas the mixture of Gly + $CaCO_3$ + CH_3CN presents the lowest transition temperature.

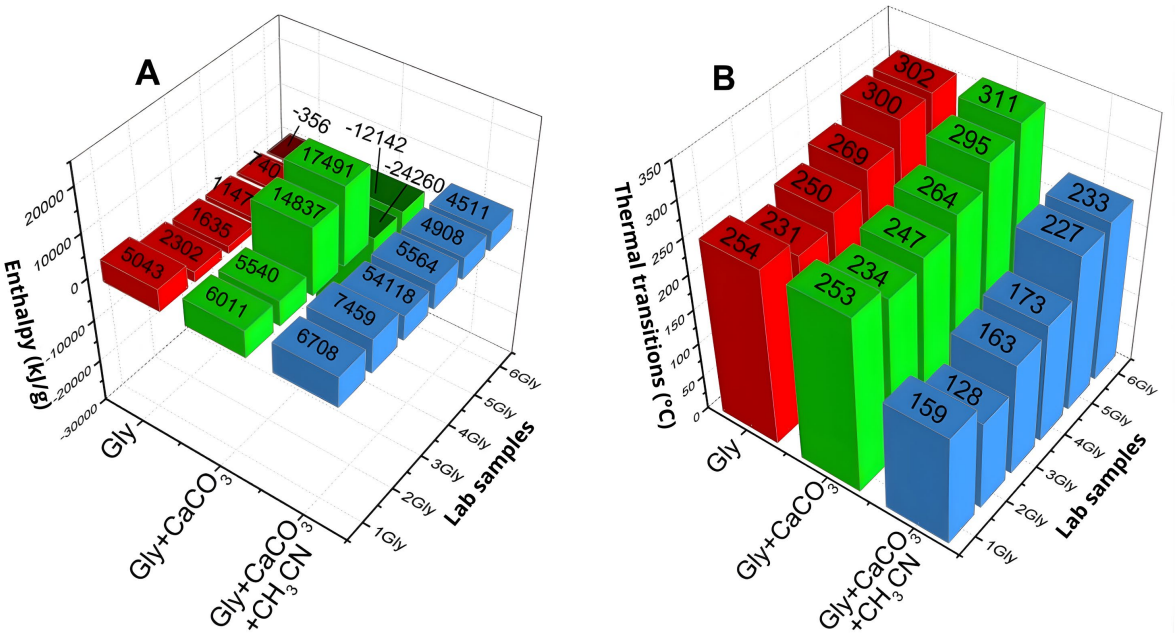

Figure 6. Behavior of enthalpies (A) and thermal transitions (B) in the different samples. The changes in enthalpy for the control glycine and the decrease in thermal transitions (lower temperatures) are noticeable when carbonate is added, and this effect is more pronounced with acetonitrile (in B). Generally speaking, the thermal transitions are more stable with increasing molecular mass.

On the other hand, the experiments in Differential Scanning Calorimetry (DSC) with exposure to UV-C irradiation (Figure 7) demonstrated significant changes in the transition temperature distribution of samples containing CH_3CN when exposed to UV-C radiation. Without UV-C, the endothermic transitions occurred between approximately 95˚C and 100˚C; however, exposure shifted this range to approximately 240˚C to 320˚C, suggesting that radiation enhances the synthesis of these materials. Notably, the samples with 5Gly exhibited atypical endothermic and exothermic behavior post-UV-C exposure. Additionally, the CH_3CN samples exhibited a destabilization effect upon UV-C irradiation (Figure 8), suggesting that acetonitrile may compromise the structural integrity, which has implications for the chemical evolution processes in glycines and carbonates in environments such as Titan and Early Earth. The distinct thermograms obtained from UV-C-exposed samples further support the notion that UV-C radiation can catalyze organic reactions.

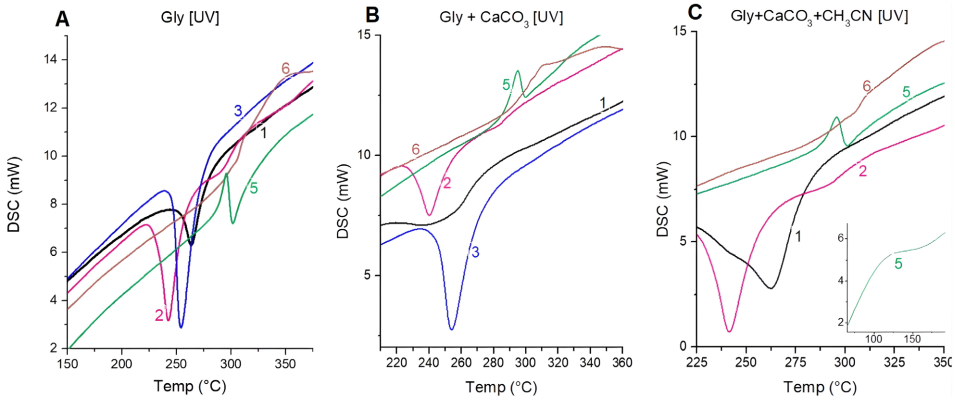

Figure 7. Differential scanning calorimetry plots of the different glycine samples are shown in colored curves, from 1Gly to 6Gly, according to their oligomers (A), with $CaCO_3$ (B), and CH_3CN (C) after exposure to UV-C radiation over two 3-hour intervals. Thermal transitions are observed at lower and lower temperatures. For graph C, a box is shown where a thermal transition outside the expected values is observed, as it occurs at approximately 125˚C, indicating instability of the reaction with acetonitrile.

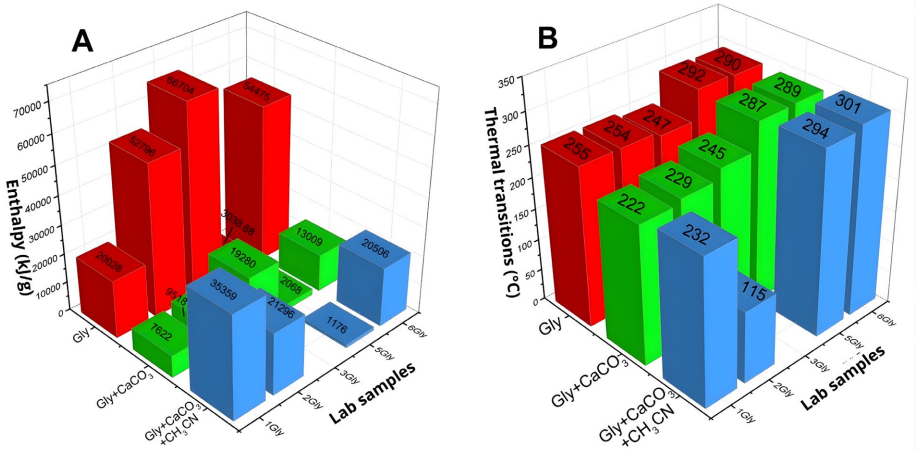

Figure 8. Behavior of the enthalpies (A) and thermal transitions (B) of the samples exposed to UV-C radiation. Contrary to the behavior shown in Figure 6, the values of enthalpy changes are considerably higher when acetonitrile is added. Likewise, it can be observed that the thermal transitions do not exhibit an abrupt change between those exposed to radiation and those not exposed, indicating that stability is maintained.

The study results, as determined by Fourier-Transform Infrared Spectroscopy (FTIR), are supported by Narayana Moolya *et al.* (2005), who identified various chemical groups in the samples, revealing the presence of new compounds following UV-C irradiation. Furthermore, infrared spectrogram analysis demonstrated a consistent increase in bands between 1700 cm^{-1} and 1500 cm^{-1}, corresponding to amides I and II, indicating the oligomerization of amino acids in both control and irradiated samples. Additionally, a comparative analysis of the spectra revealed a significant increase in intensity, indicating higher molecular diversity in irradiated samples (**Figure 9**). The most important spectral bands were attributed to glycine in conjunction with calcium carbonate and acetonitrile.

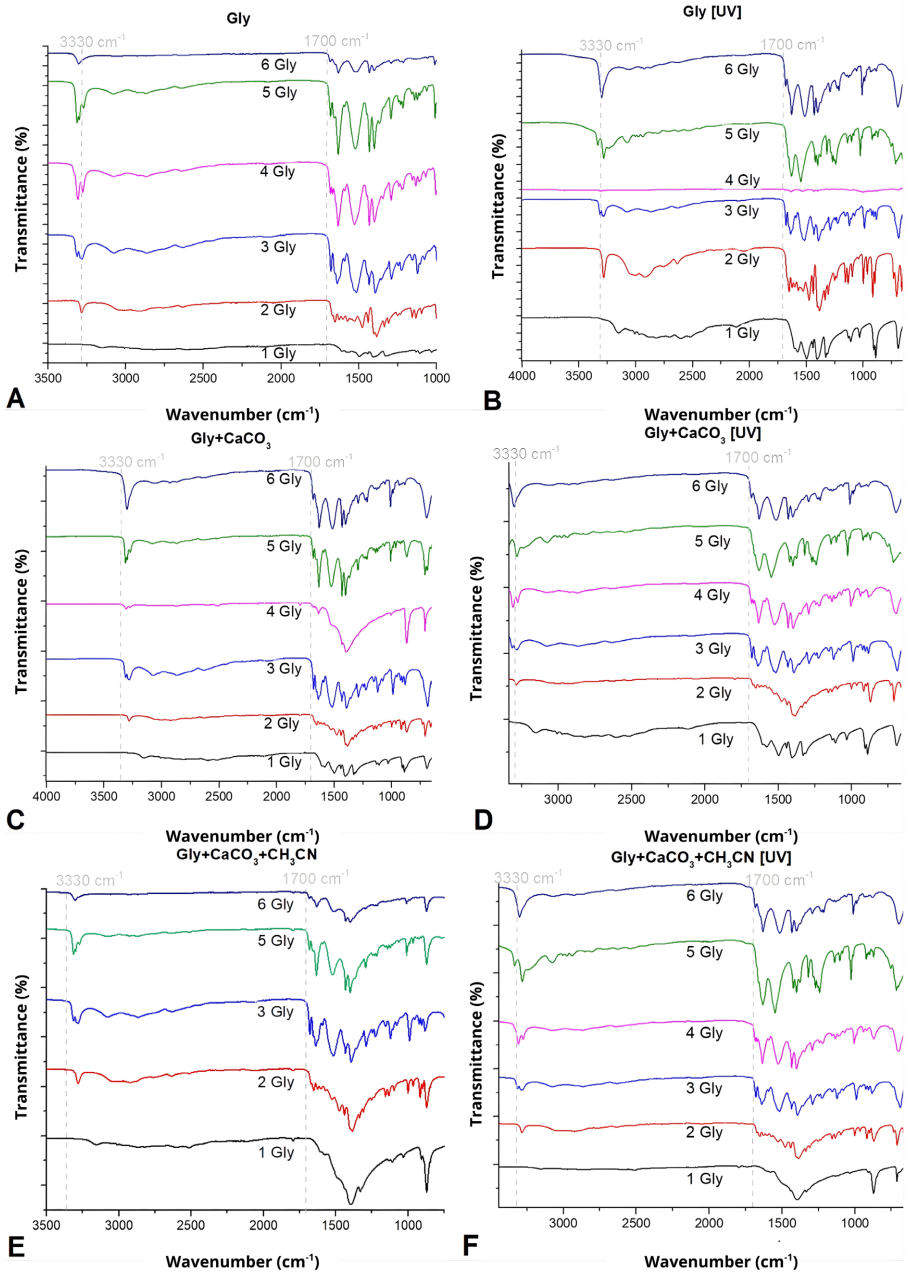

Figure 9. FTIR spectra of control and UV-C-irradiated samples. (A) Control glycines. (B) Irradiated glycins. (C) Control calcium carbonate glycines. (D) Irradiated calcium carbonate glycins. (E) Control calcium carbonate and acetonitrile glycines. (F) Irradiated calcium carbonate and acetonitrile glycines.

3.4. Attenuated Total Reflectance Fourier-Transform Infrared Spectroscopy ATR-FTIR

For this study, those compounds in the bands 3330 cm^{-1} and 1700 - 1500 cm^{-1} based on the absorption rate denoted in the band yielded by FTIR (Chandrajith & Marapana, 2018) are considered as the central vibrational frequency: 3300 - 3200 cm^{-1} (indicate the O-H bond); 3000 - 2900 cm^{-1} (correspond to C-H bonds); 1700 cm^{-1} (attributed to C=O bonds); 1100 - 1000 cm^{-1} (assign C-O bonds).

We could correlate the bands obtained for 5 Gly and 6 Gly (more stable) with the presence of the following compounds (Barth, 2007): 5 Gly [Band 1605 cm^{-1}] for arginine, lysine, aspartic acid [deprotonated], phenylalanine; 5 Gly [Band 1500 cm^{-1}] for alanine, lysine [crystalline state or salts], phenylalanine; 6 Gly [Band 1665 cm^{-1}] for Alanine and Proline [leaves], tryptophan, alanine and Proline [β-sheets], aspartic acid [salts]. These assignments are based on spectral similarities between the observed bands and characteristic vibrational modes reported for these amino acids.

It is crucial to consider the possible presence of lipids, as they, like proteins, are precursors to protein membranes. To find lipid bands in the FTIR results, we used the second derivative of the spectrogram of the samples with carbonate and acetonitrile once they had been subjected to UV-C radiation to identify the lipid bands present in the spectrum, as we had seen previously, which were identified in 3330 cm^{-1} for C-H vibrations, 1700 cm^{-1} to C=O bonds and 1000 cm^{-1} for C-O bonds. The evidence of this change between non-irradiated and irradiated samples is shown in **Figure 10**, where the second derivatives demonstrate the intervals in the lipid bands. We can see a significant diversity of bands once irradiation is introduced.

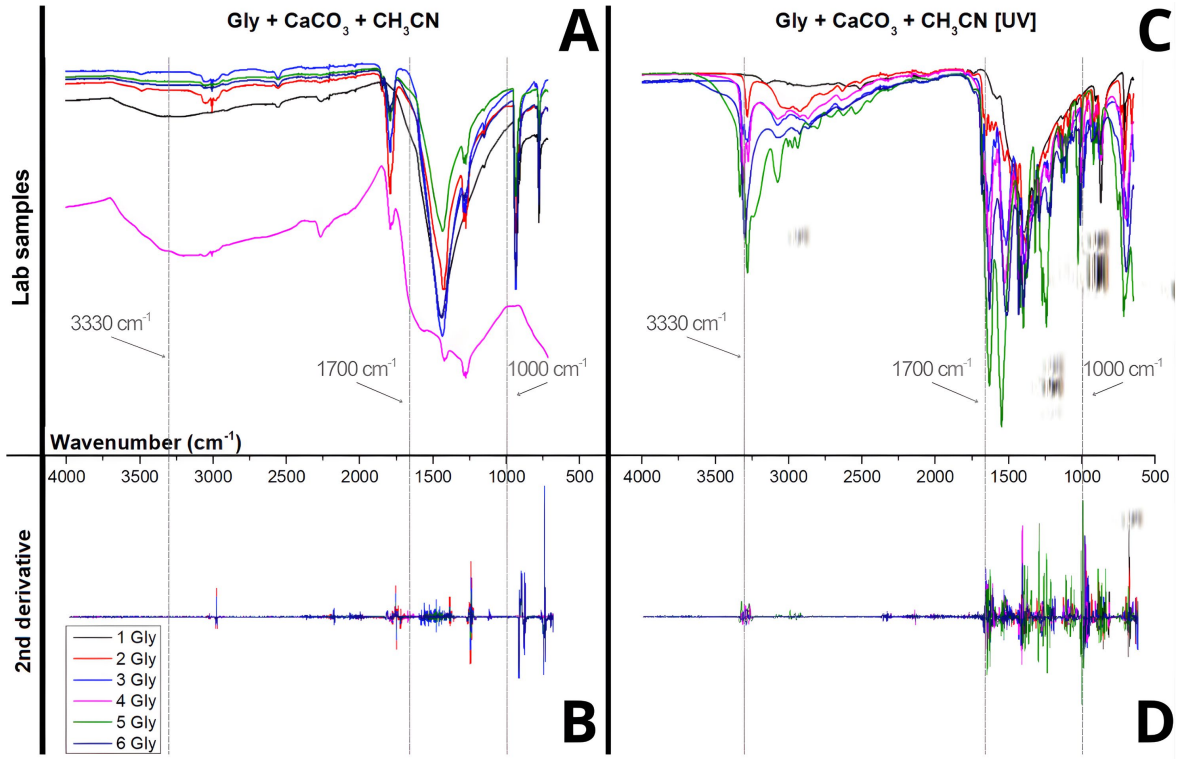

Figure 10. Spectra of samples with carbonate and acetonitrile without irradiation (A) and with irradiation (C), and their corresponding second derivative. In contrast, the second derivative of non-irradiated samples (B) shows less band diversity than the second derivative with radiation.

4. DISCUSSION

Our findings, which demonstrate the formation and increased molecular mass of glycine oligomers in the presence of $CaCO_3$ and CH_3CN under simulated prebiotic conditions, allow us to speculate on the

emergence of proto-mechanical functions in these simple systems. In this context, it is insightful to compare the complex organic materials we synthesized with the tholins known to form in Titan's atmosphere. Tholins are amorphous, aerosol-like polymers that serve as a diverse chemical reservoir of amino acids, from which we consider the glycines used in the experiment to precipitate. It has an apparent propensity to form specific secondary structures such as beta-sheets and alpha-helices. This is a fundamental condition for a molecule to act as a machine, as mechanical movement often involves a reversible conformational change.

The significant decrease in thermal stability (down to 80˚C) observed in systems containing $CaCO_3$ and CH_3CN suggests that these structures have gained flexibility, a property that allows molecular machines to "change shape" in response to stimuli.

Second, the elevated dipole moments and potential catalytic reactivity imply that these oligomers could act as systems that transform energy. In a prebiotic environment, energy could come from sources such as UV-C radiation, which our experiments show enhances amide formation. This conversion of light or chemical energy into reactivity is an operational principle analogous to that of modern molecular machines.

Finally, the increased stability of glycine compounds mediated by the $CaCO_3$-CH_3CN interaction is fundamental. Natural molecular machines are not inherently stable, and our system demonstrates how a specific mineralogical environment could have stabilized the first oligomers with functional potential. Therefore, we propose that the oligomers synthesized in our study represent a key link in molecular evolution: structures that possessed the conformational versatility, energy conversion capability, and chemical reactivity necessary to give rise to the first molecular systems capable of quasi-mechanical movement, laying the foundation for the origin of life.

5. CONCLUSION

The preliminary experiments involving CH_3CN suggest its crucial role in prebiotic chemistry and molecular evolution. The findings indicate that CH_3CN facilitates the generation of complex compounds from simpler ones and that the synthesis mechanism is associated with reduced thermal stability. The study also highlights the similarities between molecular evolution processes between Titan and Early Earth. The preliminary use of CH_3CN in experiments suggests its critical role in prebiotic chemistry and molecular evolution, specifically in forming more complex compounds and correlating with synthesis mechanisms and reduced thermal stability. This research indicates a similar molecular evolution pathway on Titan and Early Earth. Furthermore, the formation of peptide compounds featuring secondary structures is notably influenced by $CaCO_3$ crystals and CH_3CN in environments similar to those of Titan and Early Earth. These findings highlight the shared environmental characteristics of Titan and Early Earth that facilitate the synthesis of complex molecules pertinent to prebiotic evolution. This study focused on characterizing complex molecules derived from glycine and its oligomers through simple synthesis across various physicochemical environments. Ongoing research seeks to identify the physicochemical conditions that could lead to the prebiotic synthesis of compounds exhibiting emerging properties, potentially resembling primitive molecular machines.

ACKNOWLEDGEMENTS

This work was funded by the Programa de Apoyo a Proyectos de Investigación e Innovación Tecnológica (Program for Supporting Research and Technological Innovation Projects) of the UNAM (National Autonomous University of Mexico) [Project number: UNAM-DGAPA-PAPIIT-IN214825] and Secretaría de Ciencia, Humanidades, Tecnología e Innovación (Secretariat of Science, Humanities, Technology and Innovation) [Project number: SECIHTI CF2023-I-2604].

CONFLICTS OF INTEREST

The authors declare no conflicts of interest regarding the publication of this paper.

REFERENCES

1. Ángeles-Camacho, J., Morales, P., Pizarro, W., Macías, V. and Avalos, E. (2017) Los Aminoácidos en el cuerpo humano. *RECIMUNDO*: *Revista Científica de la Investigación y el Conocimiento*, **1**, 379-391.
2. Herrera, A.L. (1942) A New Theory of the Origin and Nature of Life. *Science*, **96**, 14. https://doi.org/10.1126/science.96.2479.14
3. Miller, S.L. (1953) A Production of Amino Acids under Possible Primitive Earth Conditions. *Science*, **117**, 528-529. https://doi.org/10.1126/science.117.3046.528
4. Sousa, F.L., Thiergart, T., Landan, G., Nelson-Sathi, S., Pereira, I.A.C., Allen, J.F., *et al.* (2013) Early Bioenergetic Evolution. *Philosophical Transactions of the Royal Society B*: *Biological Sciences*, **368**, Article ID: 20130088. https://doi.org/10.1098/rstb.2013.0088
5. Porco, C.C., Baker, E., Barbara, J., Beurle, K., Brahic, A., Burns, J.A., *et al.* (2005) Imaging of Titan from the Cassini Spacecraft. *Nature*, **434**, 159-168. https://doi.org/10.1038/nature03436
6. Lunine, J.I. and Hörst, S.M. (2011) Organic Chemistry on the Surface of Titan. *Rendiconti Lincei*, **22**, 183-189. https://doi.org/10.1007/s12210-011-0130-8
7. Edison, A.S. (2001) Linus Pauling and the Planar Peptide Bond. *Nature Structural Biology*, **8**, 201-202. https://doi.org/10.1038/84921
8. Draganíc, I.G. (2000) The Role of Radiation in the Origin and Evolution of Life. *Radiation Research*, **154**, 353-353. https://doi.org/10.1667/0033-7587(2000)154[0353:trorit]2.0.co;2
9. Spinks, J.W.T. and Woods, R.J. (1990) An Introduction to Radiation Chemistry. 3rd Edition, Wiley.
10. Angeles-Camacho, E., Cruz-Castañeda, J., Meléndez, A., Colín-García, M., Cruz, K.C.d.l., Ramos-Bernal, S., *et al.* (2020) Potential Prebiotic Relevance of Glycine Single Crystals Enclosing Fluid Inclusions: An Experimental and Computer Simulation with Static Magnetic Fields. *Advances in Biological Chemistry*, **10**, 140-156. https://doi.org/10.4236/abc.2020.105011
11. Powner, M.W., Gerland, B. and Sutherland, J.D. (2009) Synthesis of Activated Pyrimidine Ribonucleotides in Prebiotically Plausible Conditions. *Nature*, **459**, 239-242. https://doi.org/10.1038/nature08013
12. Coustenis, A. (2016) Titan's Organic Chemistry: A Planetary-Scale Laboratory to Study Primitive Earth. *Metode Science Studies Journal*, No. 6, 175-181. https://doi.org/10.7203/metode.6.4999
13. Li, Y. (2022) Minerals as Prebiotic Catalysts for Chemical Evolution Towards the Origin of Life. In: René, M., Ed., *Mineralogy*, IntechOpen, 1-18. https://doi.org/10.5772/intechopen.102389
14. Oosawa, F. and Hayashi, S. (1986) The Loose Coupling Mechanism in Molecular Machines of Living Cells. *Advances in Biophysics*, **22**, 151-183. https://doi.org/10.1016/0065-227x(86)90005-5
15. Cepelewicz, J. (2017) Life's First Molecule Was Protein, Not RNA, New Model Suggests. Quanta Magazine. https://www.scientificamerican.com/article/life-rsquo-s-first-molecule-was-protein-not-rna-new-model-suggests/
16. Raulin, F. (2014) Tholins. In: Amils, R., *et al.*, Eds., *Encyclopedia of Astrobiology*, Springer, 1-4. https://doi.org/10.1007/978-3-642-27833-4_1588-4
17. Cunha de Miranda, B., Garcia, G.A., Gaie-Levrel, F., Mahjoub, A., Gautier, T., Fleury, B., *et al.* (2016) Molecular Isomer Identification of Titan's Tholins Organic Aerosols by Photoelectron/Photoion Coincidence Spectroscopy Coupled to VUV Synchrotron Radiation. *The Journal of Physical Chemistry A*, **120**, 6529-6540. https://doi.org/10.1021/acs.jpca.6b03346
18. Waite, J.H., Young, D.T., Cravens, T.E., Coates, A.J., Crary, F.J., Magee, B., *et al.* (2007) The Process of Tholin Formation in Titan's Upper Atmosphere. *Science*, **316**, 870-875. https://doi.org/10.1126/science.1139727

19. Ida, N. (2004) Engineering Electromagnetics. 2nd Edition, Springer.
20. Keszthelyi, S., Gibicsar, S., Binder, A., Somfalvi-Tóth, K. and Pál-Fám, F. (2024) Impact of UV-C Irradiation on Storage Pests with Different Ecological Functions and the Viability of the Treated Grains. *Journal of Plant Protection Research*, **64**, 384-393. https://doi.org/10.24425/jppr.2024.152885
21. Sulaiman, A.H., Achilleos, N., Bertucci, C., Coates, A., Dougherty, M., Hadid, L., *et al.* (2021) Enceladus and Titan: Emerging Worlds of the Solar System. *Experimental Astronomy*, **54**, 849-876. https://doi.org/10.1007/s10686-021-09810-z
22. Marty, B. (2012) The Origins and Concentrations of Water, Carbon, Nitrogen and Noble Gases on Earth. *Earth and Planetary Science Letters*, **313**, 56-66. https://doi.org/10.1016/j.epsl.2011.10.040
23. Saxena, P.P. (2007) On the Possibility of Gly and Ala Amino Acids on Titan. *Bulletin of the Astronomical Society of India*, **35**, 15-21. http://www.ncra.tifr.res.in/~basi/07March/35152007.pdf
24. Cable, M.L., Vu, T.H., Malaska, M.J., Maynard-Casely, H.E., Choukroun, M. and Hodyss, R. (2020) Properties and Behavior of the Acetonitrile-Acetylene Co-Crystal under Titan Surface Conditions. *ACS Earth and Space Chemistry*, **4**, 1375-1385. https://doi.org/10.1021/acsearthspacechem.0c00129
25. Coustenis, A. (2014) Titan. In: Spohn, T., Breuer, D. and Johnson, T.V., Eds., *Encyclopedia of the Solar System*, Elsevier, 831-849. https://doi.org/10.1016/b978-0-12-415845-0.00038-4
26. McKee, T. (2014) Bioquímica, las bases moleculares de la vida, Cuarta. McGraw-Hill.
27. Lunine, J.I. (2009) Titan as an Analog of Earth's Past and Future. *The European Physical Journal Conferences*, **1**, 267-274. https://doi.org/10.1140/epjconf/e2009-00926-7
28. Cnossen, I., Sanz-Forcada, J., Favata, F., Witasse, O., Zegers, T. and Arnold, N.F. (2007) Habitat of Early Life: Solar X-Ray and UV Radiation at Earth's Surface 4-3.5 Billion Years Ago. *Journal of Geophysical Research*: *Planets*, **112**, E02008. https://doi.org/10.1029/2006je002784
29. Mitchell, K.L. ,*et al.* (2008) What Is Infrared Spectroscopy? Fundamentals & Applications. *Geophysical Research Letters*, **35**, 2007GL032118.
30. Neish, C.D., Kirk, R.L., Lorenz, R.D., Bray, V.J., Schenk, P., Stiles, B.W., *et al.* (2013) Crater Topography on Titan: Implications for Landscape Evolution. *Icarus*, **223**, 82-90. https://doi.org/10.1016/j.icarus.2012.11.030
31. Fried, S.D., Fujishima, K., Makarov, M., Cherepashuk, I. and Hlouchova, K. (2022) Peptides before and during the Nucleotide World: An Origins Story Emphasizing Cooperation between Proteins and Nucleic Acids. *Journal of The Royal Society Interface*, **19**, Article ID: 20210641. https://doi.org/10.1098/rsif.2021.0641
32. Polanski, J. (2009) Chemoinformatics. In: Brown, S.D., Tauler, R. and Walczak, B., Eds., *Comprehensive Chemometrics*, Elsevier, 459-506. https://doi.org/10.1016/b978-044452701-1.00006-5
33. Sandoval Quintana, A., Rodriguez Sandoval, E. and Fernandez Quintero, F. (2005) Aplicación del análisis por calorimetría diferencial de barrido (DSC) para la caracterización de las modificaciones del almidón. *Dyna*, **72**, 45-53.
34. Schrader, B. (1995) Infrared and Raman Spectroscopy: Methods and Applications. Wiley.
35. Rieppo, L., Saarakkala, S., Närhi, T., Helminen, H.J., Jurvelin, J.S. and Rieppo, J. (2012) Application of Second Derivative Spectroscopy for Increasing Molecular Specificity of Fourier Transform Infrared Spectroscopic Imaging of Articular Cartilage. *Osteoarthritis and Cartilage*, **20**, 451-459. https://doi.org/10.1016/j.joca.2012.01.010
36. Roy, S., Chatterjee, A., Bal, S. and Das, D. (2022) Cross β Amyloid Nanotubes Demonstrate Promiscuous Catalysis in a Chemical Reaction Network via Co-Option. *Angewandte Chemie International Edition*, **61**, e202210972. https://doi.org/10.1002/anie.202210972